arXiv:cond-mat/9811261v1 [cond-mat.supr-con] 17 Nov 1998

Journal of Superconductivity, Vol. ??, No. ?, 1999

Stripes, Electron-Like and Polaron-Like Carriers, and High-T_c in the Cuprates

J. Ashkenazi[1]

Received 4 November 1998

Both "large-U" and "small-U" orbitals are used to study the electronic structure of the high-T_c cuprates. A striped structure with three types of carriers are induced, polaron-like "stripons" which carry charge, "quasielectrons" which carry both charge and spin, and "svivons" which carry spin and lattice distortion. Anomalous physical properties of the cuprates are derived, and specifically the systematic behavior of the resistivity, Hall constant, and thermoelectric power. Transitions between pair states of quasielectrons and stripons drive high-temperature superconductivity.

KEY WORDS: high-T_c superconductivity, stripes, transport properties, mechanism.

1. INTRODUCTION

Evidence is growing [1] that the CuO_2 planes in the high-T_c cuprates possess a static or a dynamic striped structure. The physical properties of these materials, and specifically their transport properties are characterized by intriguing anomalies suggesting the inadequacy of the Fermi-liquid scenario, and/or the coexistence of itinerant and almost localized (or polaron-like) carriers.

First-principles electronic structure studies [2] suggest that realistic theoretical models of the electrons in the vicinity of the Fermi level ($E_{\rm F}$) should take into account both "large-U" and "small-U" orbitals [3]. Let us denote the fermion creation operator of a small-U electron in band ν, spin σ, and wave vector $\mathbf{k}$ by $c^\dagger_{\nu\sigma}(\mathbf{k})$.

2. AUXILIARY SPACE

Let us treat the large-U orbitals by the "slave-fermion" method [4]. A large-U electron in site i and spin σ is then created by $d^\dagger_{i\sigma} = e^\dagger_i s_{i,-\sigma}$, if it is in the "upper-Hubbard-band", and by $d^{\prime\dagger}_{i\sigma} = \sigma s^\dagger_{i\sigma} h_i$, if it is in a Zhang-Rice-type "lower-Hubbard-band". Here e_i and h_i are ("excession" and "holon") fermion operators, and $s_{i\sigma}$ are ("spinon") boson operators. The constraint:

$$e^\dagger_i e_i + h^\dagger_i h_i + \sum_\sigma s^\dagger_{i\sigma} s_{i\sigma} = 1 \quad (1)$$

should be satisfied in every site.

Within an auxiliary Hilbert space a chemical-potential-like Lagrange multiplier is introduced to impose the constraint on the average. Physical observables are then projected into the physical space by taking appropriate combinations of Green's functions of the auxiliary space. Since the time evolution of Green's functions is determined by the Hamiltonian which obeys the constraint rigorously, effects of constraint violation may result only from the approximations applied treating these Green's functions. *E.g.*, within the "spin-charge separation" approximation two-particle spinon-holon Green's functions are decoupled into products of one-(auxiliary)-particle Green's functions.

The spinon states are diagonalized by applying the Bogoliubov transformation:

$$s_\sigma(\mathbf{k}) = \cosh(\xi_{\sigma\mathbf{k}})\zeta_\sigma(\mathbf{k}) + \sinh(\xi_{\sigma\mathbf{k}})\zeta^\dagger_{-\sigma}(-\mathbf{k}). \quad (2)$$

The Bose operators $\zeta^\dagger_\sigma(\mathbf{k})$ create spinon states with "bare" energies $\epsilon^\zeta(\mathbf{k})$ which have a V-shape zero minimum at $\mathbf{k} = \mathbf{k}_0$, whose value is either $(\frac{\pi}{2a}, \frac{\pi}{2a})$ or $(\frac{\pi}{2a}, -\frac{\pi}{2a})$. Bose condensation results in antiferromagnetism (AF), and the spinon reciprocal lattice is extended by adding the wave vector $\mathbf{Q} = 2\mathbf{k}_0$.

The slave-fermion method is known to describe well an AF state. Since within this method AF order is obtained by the Bose condensation of spinons, the decoupling of two-particle spinon-spinon Green's

[1] Physics Department, University of Miami, P.O. Box 248046, Coral Gables, FL 33124, U.S.A.

functions, relevant for physical spin processes, does not harm the treatment of spin-spin correlations.

3. STRIPES AND QUASIPARTICLES

Theoretically, a lightly doped AF plane tends to separate into a "charged" phase and an AF phase. A preferred structure under long-range Coulomb repulsion is [5] of frustrated stripes of these phases. Experiment [6] confirms such a scenario, and neutron-scattering measurements [7] indicate at least in certain cases a structure where narrow charged stripes form antiphase domain walls separating wider AF stripes. Growing evidence [1] supports the assumption that such a structure exists, at least dynamically, in all the superconducting cuprates.

Since the spin-charge separation approximation is valid in one-dimension, it should apply for holons (excessions) within the charged stripes, and they are referred to as "stripons". They carry charge, but not spin. We denote their fermion creation operators by $p_{\mu}^{\dagger}(\mathbf{k})$, and their bare energies by $\epsilon_{\mu}^{p}(\mathbf{k})$.

It is evident [1] that the stripes in the cuprates are far from being perfect. Even when they are not dynamic, one expects them to be defected and "frustrated", and to consist of disconnected segments. Such a structure is fatal for itinerancy in one-dimension, and it is reasonable to choose localized states as the starting point for the stripon states.

Other carriers (of both charge and spin) result from the hybridization (in the auxiliary space) of small-U electrons and coupled holon-spinons (excession-spinons) within the AF stripes. We refer to these carriers as "Quasi-electrons" (QE's), and denote their fermion creation operators by $q_{\iota\sigma}^{\dagger}(\mathbf{k})$. Their bare energies $\epsilon_{\iota}^{q}(\mathbf{k})$ form quasi-continuous ranges of bands crossing E_{F} over ranges of the Brillouin zone (BZ).

4. SPECTRAL FUNCTIONS

The physical observables are evaluated using electrons Green's functions. Expressions are derived where the observables are expressed in terms of the auxiliary space spectral functions $A_{\iota}^{q}(\mathbf{k},\omega)$, $A_{\lambda}^{\zeta}(\mathbf{k},\omega)$, and $A_{\mu}^{p}(\mathbf{k},\omega)$, of the QE's, spinons, and stripons, respectively.

The quasiparticle fields are strongly coupled to each other due to hopping and hybridization terms of the Hamiltonian. This coupling can be expressed through an effective Hamiltonian term whose parameters can be in principle derived self-consistently from the original Hamiltonian. It has the form:

$$\mathcal{H}' = \frac{1}{\sqrt{N}} \sum_{\iota\mu\lambda\sigma} \sum_{\mathbf{k},\mathbf{k}'} \Big\{ \sigma \epsilon_{\iota\mu\lambda\sigma}^{qp}(\mathbf{k}',\mathbf{k}) q_{\iota\sigma}^{\dagger}(\mathbf{k}) p_{\mu}(\mathbf{k}') \times \big[\cosh(\xi_{\lambda\sigma,(\mathbf{k}-\mathbf{k}')}) \zeta_{\lambda\sigma}(\mathbf{k}-\mathbf{k}') + \sinh(\xi_{\lambda\sigma,(\mathbf{k}-\mathbf{k}')}) \zeta_{\lambda,-\sigma}^{\dagger}(\mathbf{k}'-\mathbf{k}) \big] + h.c. \Big\}, \quad (3)$$

The auxiliary space spectral functions are calculated through the standard diagrammatic technique where $\mathcal{H}'$ introduces a vertex connecting QE, stripon and spinon propagators. It turns out that the stripon bandwidth is at least an order of magnitude smaller than the QE and spinon bandwidths. Thus, by a generalized Migdal theorem one gets that "vertex corrections" are negligible, and a second-order perturbation expansion in $\mathcal{H}'$ is applicable.

Applying the diagrammatic technique, self-consistent expressions are derived for the scattering rates $\Gamma_{\iota}^{q}(\mathbf{k},\omega)$, $\Gamma_{\lambda}^{\zeta}(\mathbf{k},\omega)$, and $\Gamma_{\mu}^{p}(\mathbf{k},\omega)$, of the QE's, spinons, and stripons, respectively. For sufficiently doped cuprates the self-consistent solution has the following features:

Spinons

The spinon spectral functions behave as: $A^{\zeta}(\mathbf{k},\omega) \propto \omega$ for small ω. Thus $A^{\zeta}(\mathbf{k},\omega) b_{T}(\omega) \propto T$ for $\omega \ll T$, where $b_{T}(\omega)$ is the Bose distribution function at temperature T. Namely there is no long-range AF order (associated with the divergence in the number of spinons at $\mathbf{k} = \mathbf{k}_0$).

Stripons

The coupling between the stripon field and the other fields results in the renormalization of the localized stripon energies into a very narrow range around E_{F} (thus getting polaron-like states). Some hopping via QE-spinon states results is the onset of itineracy at low temperatures, with a bandwidth of $\sim$0.02 eV. The stripon reciprocal lattice is extended by adding wave vectors corresponding to the approximate periodicity of the striped structure.

The stripon scattering rates can be expressed as;

$$\Gamma^{p}(\mathbf{k},\omega) \propto A\omega^2 + B\omega T + CT^2. \quad (4)$$

Quasi-electrons

The QE scattering rates, resulting from their coupling to the other fields, can be approximately expressed as:

$$\Gamma^{q}(\mathbf{k},\omega) \propto \omega[b_{T}(\omega) + \tfrac{1}{2}]. \quad (5)$$

This becomes $\Gamma^{q}(\mathbf{k},\omega) \propto T$ in the limit $T \gg |\omega|$, and $\Gamma^{q}(\mathbf{k},\omega) \propto \frac{1}{2}|\omega|$ in the limit $T \ll |\omega|$, in agreement with "marginal Fermi liquid" phenomenology [8].

5. SOME PHYSICAL ANOMALIES

5.1 Lattice effects ("svivons")

As was found by Bianconi *et al.* [6] the charged stripes are characterized by LTT structure, while the AF stripes are characterized by LTO structure. Thus, in any physical process induced by $\mathcal{H}'$ (3), where a stripon transforms into a QE, or vice versa, followed by the emission/absorption of a spinon, phonons are also emitted/absorbed, and the stripons have lattice features of polarons.

The result is that a spinon propagator linked to the $\mathcal{H}'$ vertex is "dressed" by phonon propagators. We refer to such a phonon-dressed spinon as a svivon. Its propagator can be expressed as a spinon propagator multiplied by a power series of phonon propagators. As dressed spinons the svivons carry spin, but not charge; however they also "carry" lattice distortion.

5.2 Optical conductivity

The optical conductivity of the doped cuprates is characterized [9] by a Drude term and mid-IR peaks. Transitions between low energy QE states result in the Drude term. Excitations of the very low energy stripon states result in the mid-IR peaks. Such excitation can either leave a stripon in the same stripe segment, exciting spinon and phonon states, or transform a stripon into a QE-svivon state.

5.3 Spectroscopic anomalies

The electronic spectral function, measured, *e.g.*, in photoemission experiments, includes "coherent" bands, and an "incoherent" background of a comparable integrated weight. The coherent part is due to few QE bands, and the frequently observed $\sim|E-E_{\rm F}|$ bandwidth is consistent with Eq. (5). The incoherent part is due to the quasi-continuum of other QE bands, and to the stripon states (note that the spectroscopic signature of stripons is smeared over few tenths of an eV around $E_{\rm F}$ due to the accompanying svivon excitations).

The observed "Shadow bands", "extended" van Hove singularities (vHs), and normal-state pseudogaps result from the effect of the striped structure on the QE bands [10], due to the extension of the reciprocal lattice (discussed above). The vHs are extended to supply the spectral weight for the stripon states, and when the vHs are missing this transferred spectral weight causes a pseudogap in the same place in the BZ [11].

6. TRANSPORT PROPERTIES

6.1 Electric current (dc)

The electric current $\mathbf{j}$ is expressed as a sum of QE and stripon contributions $\mathbf{j}^q$ and $\mathbf{j}^p$, respectively:

$$\mathbf{j} = \mathbf{j}^q + \mathbf{j}^p. \tag{6}$$

As was discussed above, stripons transport occurs through transitions to intermediate QE-spinon states. Consequently, the expressions for the currents yield:

$$\mathbf{j}^p \cong \alpha \mathbf{j}^q, \tag{7}$$

where α is approximately T-independent. This condition is satisfied by the formation of gradients $\boldsymbol{\nabla}\mu^{\mathbf{q}}$ and $\boldsymbol{\nabla}\mu^{\mathbf{p}}$ of the QE and stripon chemical potentials (respectively) in the presence of an electric field. The constraint on the number of electrons imposes:

$$N^q \boldsymbol{\nabla}\mu^{\mathbf{q}} + \mathbf{N^p} \boldsymbol{\nabla}\mu^{\mathbf{p}} = \mathbf{0}, \tag{8}$$

where N^q and N^p are, respectively, the contributions of QE's and stripons to the electrons density of states at $E_{\rm F}$.

6.2 Electrical conductivity and Hall constant

The Kubo formalism is applied to derive expressions for the dc conductivity and Hall constant in terms of Green's functions. Such expressions are based on diagonal and non-diagonal conductivity QE terms σ_{xx}^{qq} and σ_{xy}^{qqq}, stripon terms σ_{xx}^{pp} and σ_{xy}^{ppp}, and mixed terms σ_{xy}^{qqpp}.

The currents in an electric field $\mathbf{E}$ are expressed as:

$$j_x^q = \sigma_{xx}^{qq} \mathcal{E}_x^q, \qquad j_x^p = \sigma_{xx}^{pp} \mathcal{E}_x^p, \tag{9}$$

where

$$\boldsymbol{\mathcal{E}}^{\mathbf{q}} = \mathbf{E} + \frac{\boldsymbol{\nabla}\mu^{\mathbf{q}}}{\rm e}, \qquad \boldsymbol{\mathcal{E}}^{\mathbf{p}} = \mathbf{E} + \frac{\boldsymbol{\nabla}\mu^{\mathbf{p}}}{\rm e}. \tag{10}$$

Using Eqs. (8), (10), one can express:

$$\mathbf{E} = \frac{N^q \boldsymbol{\mathcal{E}}^{\mathbf{q}} + \mathbf{N^p} \boldsymbol{\mathcal{E}}^{\mathbf{p}}}{\mathbf{N^q} + \mathbf{N^p}}, \tag{11}$$

and since

$$j_x^q + j_x^p = j_x = \frac{E_x}{\rho_x}, \tag{12}$$

the resistivity in the x- direction ρ_x can be expressed as:

$$\rho_x = \frac{1}{(N^q + N^p)(1+\alpha)} \Big(\frac{N^q}{\sigma_{xx}^{qq}} + \frac{\alpha N^p}{\sigma_{xx}^{pp}} \Big). \tag{13}$$

Similarly, the Hall constant $R_{\rm H} = E_y/j_x H$ can be expressed as

$$R_{\rm H} = \frac{\rho_x}{\cot\theta_{\rm H}}, \tag{14}$$

where

$$\frac{1+\alpha}{\cot\theta_{\rm H}} = \frac{\sigma_{xy}^{qqq} + \sigma_{xy}^{qqpp}}{\sigma_{xx}^{qq}} + \frac{\alpha(\sigma_{xy}^{ppp} + \sigma_{xy}^{qqpp})}{\sigma_{xx}^{pp}}. \tag{15}$$

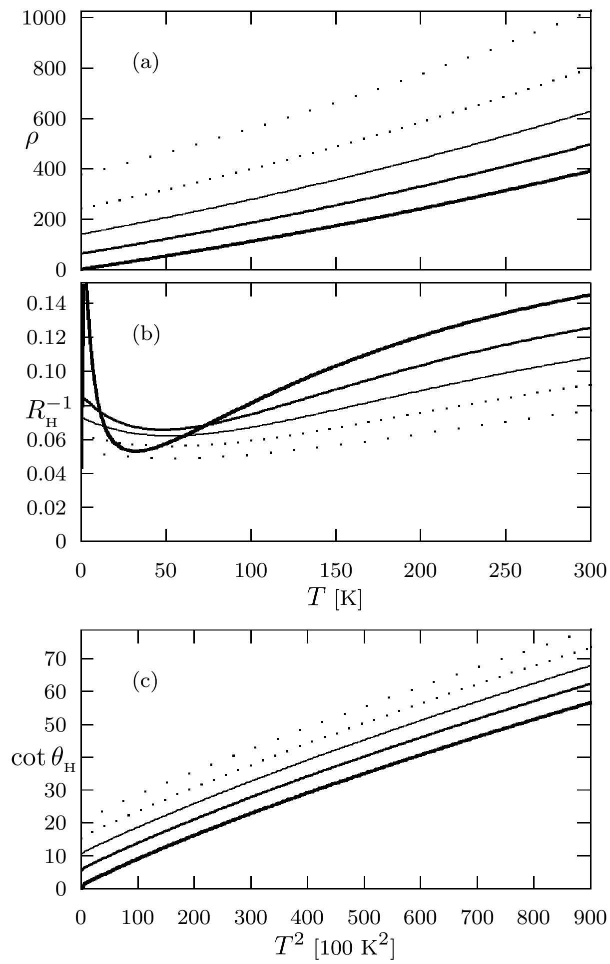

FIG. 1. The resistivity (a), inverse Hall constant (b), and $\cot\theta_{\rm H}$ (c), in arbitrary unit, for parameter values: A=1,7,13,19,25; B=.001; C=1; D=0,50,100,150,200; N=1,.9,.8,.7,.6; Z=2. The first value corresponds to the thickest lines.

In order to find the temperature dependencies of the transport quantities we apply our results for the scattering rates Γ^q and Γ^p, given in Eqs. (4), (5), to which we add temperature-independent impurity scattering terms. Consequently one can express the temperature dependencies of the conductivity terms using parameters A, B, C, D, N, and Z, as follows:

$$\sigma_{xx}^{qq} \propto \frac{1}{D+CT}, \tag{16}$$

$$\sigma_{xx}^{pp} \propto \frac{1}{A+BT^2}, \tag{17}$$

$$\sigma_{xy}^{qqq} \propto \frac{1}{(D+CT)^2}, \tag{18}$$

$$\sigma_{xy}^{ppp} \propto \frac{1}{(A+BT^2)^2}, \tag{19}$$

$$\sigma_{xy}^{qqpp} \propto \frac{1}{(D+CT)(A+BT^2)}. \tag{20}$$

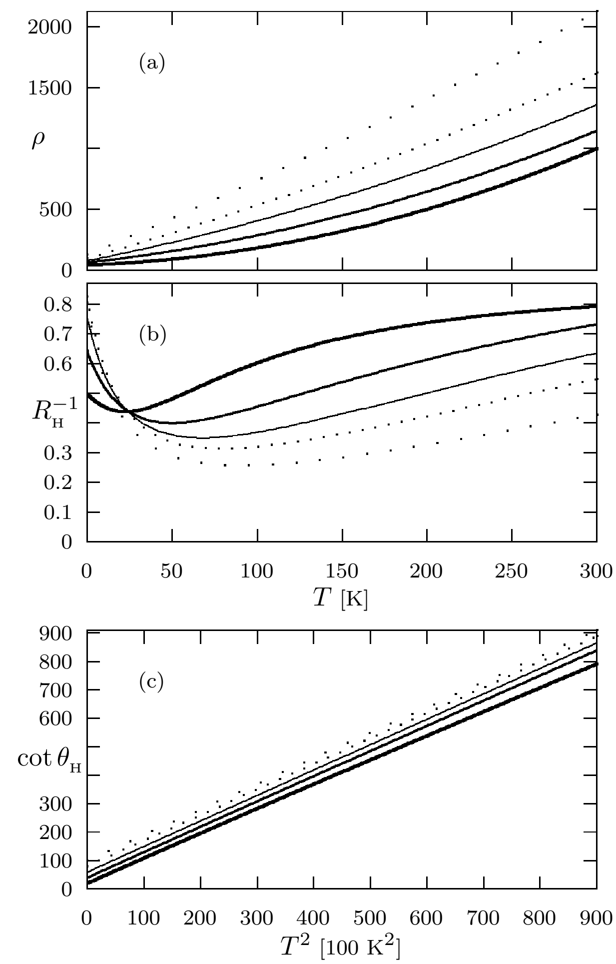

FIG. 2. The resistivity (a), inverse Hall constant (b), and $\cot\theta_{\rm H}$ (c), in arbitrary unit, for parameter values: A=20,40,60,80,100; B=.01; C=.5,2,5,10,20; D=20,40,80,160,320; N=1,1.3,1.8,2.5,3.4; Z=.01. The first value corresponds to the thickest lines.

The transport quantities are then expressed as:

$$\rho_x \cong \frac{D + CT + A + BT^2}{N}, \tag{21}$$

$$\frac{1}{\cot\theta_{\rm H}} \cong \frac{Z}{D + CT} + \frac{1}{A + BT^2}. \tag{22}$$

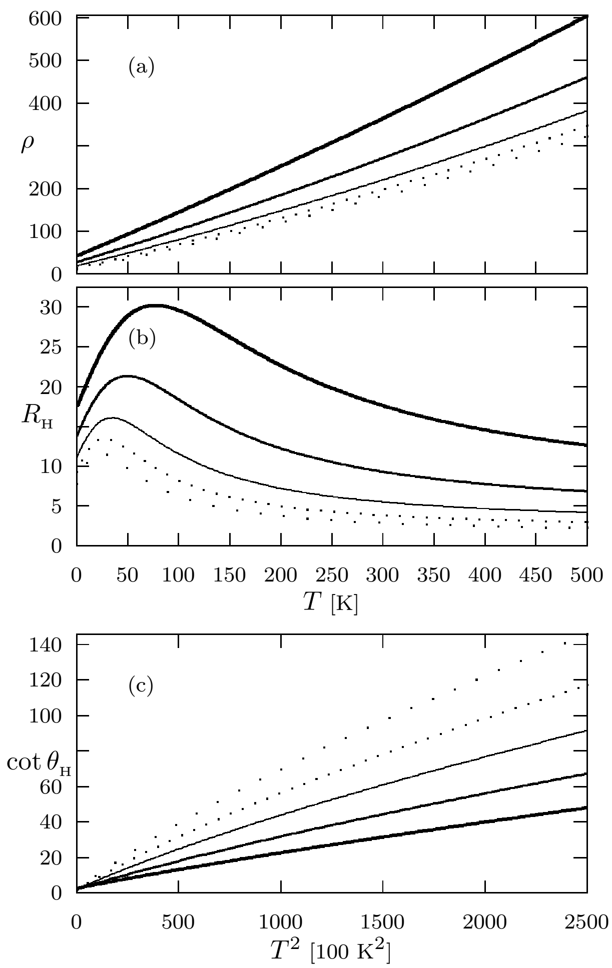

FIG. 3. The resistivity (a), Hall constant (b), and $\cot\theta_{\rm H}$ (c), in arbitrary unit, for parameter values: A=3,2.4,2,1.7,1.5; B=.00025,.0004,.0006,.0008,.001; C=1,1.1,1.3,1.6,2; D=40; N=1,1.5,2.2,3,4; Z=3. The first value corresponds to the thickest lines.

These expressions reproduce the systematic behavior of the transport quantities in different cuprates, except for the effect of the pseudogap in underdoped cuprates, ignored here. Results for sets of parameters corresponding to data in $YBa_2Cu_{3-x}Zn_xO_7$ [12], $Tl_2Ba_2CuO_{6+\delta}$ [13], and $La_{2-x}Sr_xCuO_4$ [14], are presented in Figs. 1, 2, and 3, respectively.

The idea that ρ and $\cot\theta_{\rm H}$ are determined by different scattering rates has been first suggested by Anderson [15], and in his analysis the T^2 term is due to spinons. However, it has been observed in ac Hall effect results [16] that the energy scale corresponding to this term is of about 120 K. This energy is in agreement with the very low energies of the stripons of our analysis, and not with spinon energies (which are of tenths of an eV).

6.3 Thermoelectric Power

When both an electric field and a temperature gradient are present, one can express $\mathbf{j}^q$ and $\mathbf{j}^p$ as:

$$\mathbf{j}^q = \frac{\rm e}{T}\underline{\mathbf{L}}^{q(11)}\boldsymbol{\mathcal{E}}^{\mathbf{q}} + \underline{\mathbf{L}}^{\mathbf{q(12)}}\boldsymbol{\nabla}(\frac{\mathbf{1}}{\mathbf{T}}), \tag{23}$$

$$\mathbf{j}^p = \frac{\rm e}{T}\underline{\mathbf{L}}^{p(11)}\boldsymbol{\mathcal{E}}^{\mathbf{p}} + \underline{\mathbf{L}}^{\mathbf{p(12)}}\boldsymbol{\nabla}(\frac{\mathbf{1}}{\mathbf{T}}). \tag{24}$$

The thermoelectric power (TEP) is given by

$$\underline{\mathbf{S}} = \left[\frac{\mathbf{E}}{\boldsymbol{\nabla}\mathbf{T}}\right]_{\mathbf{j}=0}. \tag{25}$$

By Eq. (7), the condition $\mathbf{j} = 0$ for the evaluation of the TEP becomes $\mathbf{j}^q \cong \mathbf{j}^p \cong 0$.

Thus, by introducing

$$\underline{\mathbf{S}}^q = \left[\frac{\boldsymbol{\mathcal{E}}^{\mathbf{q}}}{\boldsymbol{\nabla}\mathbf{T}}\right]_{\mathbf{j}^q=0} = -\frac{1}{{\rm e}T}\frac{\underline{\mathbf{L}}^{q(12)}}{\underline{\mathbf{L}}^{q(11)}}, \tag{26}$$

$$\underline{\mathbf{S}}^p = \left[\frac{\boldsymbol{\mathcal{E}}^{\mathbf{p}}}{\boldsymbol{\nabla}\mathbf{T}}\right]_{\mathbf{j}^p=0} = -\frac{1}{{\rm e}T}\frac{\underline{\mathbf{L}}^{p(12)}}{\underline{\mathbf{L}}^{p(11)}}, \tag{27}$$

and using Eqs. (11), (23), (24), we get that the TEP can be expressed as:

$$\underline{\mathbf{S}} = \frac{N^q\underline{\mathbf{S}}^q + N^p\underline{\mathbf{S}}^p}{N^q + N^p}. \tag{28}$$

The QE bandwidths are close to an eV. Thus one gets

$$S^q \propto T, \tag{29}$$

similarly to the TEP in normal metals. On the other hand the stripon bandwidth is of order 0.02 eV. Thus one expects S^p to saturate at $T \sim 200$ K to the narrow-band result [17]:

$$S^p = \frac{k_{\rm B}}{\rm e}\ln\left[\frac{1 - n^p}{n^p}\right], \tag{30}$$

where n^p is the fractional occupation of the stripon band.

This result for the TEP is consistent with the typical behavior observed in the cuprates. Such a behavior has been parametrized as [18]:

$$S = AT + \frac{BT^\alpha}{(T+\Theta)^\alpha}. \tag{31}$$

It was found [17,19] that $S^p = 0$ (namely the stripon band is half full) for slightly overdoped cuprates.

The effect of the doping of a cuprate is [7] both to change the density of the charged stripes within a CuO_2 plane, and to change the density of carriers (stripons) within a charged stripe. It is the second type of doping effect that changes n^p. overdoping is often limited because a large density carriers in the charged stripes results in an increase of Coulomb repulsion energy.

7. MECHANISM FOR HIGH-T_c

The coupling Hamiltonian $\mathcal{H}'$ (3) provides a mechanism for high-T_c. The pairing mechanism involves transitions between pair states of QE's and stripons through the exchange of svivons. Such a mechanism has similarities to the interband pair transition mechanism proposed by Kondo [20].

The symmetry of the superconducting gap is strongly affected by the symmetry of the QE-stripon coupling through $\mathcal{H}'$, and is thus related to the symmetry of the normal-state pseudogap (also determined by QE-stripon coupling). Similarity between the **k**-space symmetries of these gaps has been observed [11].

A condition for superconductivity within the present approach is that the narrow stripon band maintains coherence between different stripe segments. Thus an upper limit for T_c is determined by the temperature where such coherence sets in.

When the stripon band is almost empty (or almost full), it can be treated in the parabolic approximation, and it is characterized by the distance $\mathcal{E}_{\rm F}$ of the Fermi level from the bottom (top) of the band at $T = 0$. Using a two-dimensional approximation one can express $\mathcal{E}_{\rm F}$ as:

$$\mathcal{E}_{\rm F} = 2\pi\hbar^2 \frac{n^*}{m^*}, \tag{32}$$

where m^* in the stripons effective mass and n^* is their density per unit area of a CuO_2 plane (note that the stripons are spinless).

Stripon coherence is energetically favorable at temperatures where there is a clear cut between occupied and unoccupied stripon band states, which is of order of $\mathcal{E}_{\rm F}/k_{\rm B}$. And this determines an upper limit for T_c:

$$k_{\rm B} T_c \lesssim \mathcal{E}_{\rm F}. \tag{33}$$

This result agrees with the "Uemura plots" [21] if the n^*/m^* ratio for stripons is approximately proportional to that for the supercurrent carriers, appearing in the expression for the London penetration depth (the supercurrent carriers are hybridized QE and stripon pairs). The "boomerang-type" behavior of the Uemura plots in overdoped cuprates [22] is understood as a transition between a band-top and a band-bottom behavior.

8. SUMMARY

The electronic structure of the high-T_c cuprates has been studied on the basis of both large-U and small-U orbitals. A striped structure and three types of carriers are obtained; polaron-like stripons carrying charge, QE's carrying charge and spin, and svivons carrying spin and lattice distortion.

Anomalous normal-state properties of the cuprates are understood, and the systematic behavior of the resistivity, Hall constant, and thermoelectric power is explained. The high-T_c mechanism is based on transitions between pair states of stripons and QE's through the exchange of svivons.

REFERENCES

1. Papers in *J. Supercond.* **10**, #4 (1997), and in this issue.
2. O. K. Andersen *et al.*, *J. Phys. Chem. Solids* **56**, 1573 (1995).
3. J. Ashkenazi, *J. Supercond.* **7**, 719 (1994); *ibid* **8**, 559 (1995); *ibid* **10**, 379 (1997).
4. S. E. Barnes, *Adv. Phys.* **30**, 801 (1980).
5. V. J. Emery, and S. A. Kivelson, *Physica C* **209**, 597 (1993).
6. A. Bianconi *et al.*, *Phys. Rev. B* **54**, 12018, (1996); *Phys. Rev. Lett.* **76** 3412 (1996).
7. J. M. Tranquada *et al.*, *Phys. Rev. B* **54**, 7489, (1996); *Phys. Rev. Lett.* **78**, 338 (1997).
8. C. M. Varma *et al.*, *Phys. Rev. Lett.* **63**, 1996 (1989).
9. D. B. Tanner, and T. Timusk, *Physical Properties of High Temperature Superconductors III*, edited by D. M. Ginsberg (World Scientific, 1992), p. 363.
10. M. I. Salkola, *et al.*, *Phys. Rev. Lett.* **77**, 155 (1996).
11. D. S. Marshall, *et al.*, *Phys. Rev. Lett.* **76**, 4841 (1996).
12. T. R. Chien, *et al.*, *Phys. Rev. Lett.* **67**, 2088 (1991).
13. Y. Kubo and T. Manako, *Physica C* **197**, 378 (1992).
14. H. Takagi, *et al.*, *Phys. Rev. Lett.* **69**, 2975 (1992); H. Y. Hwang, *et al.*, *ibid.* **72**, 2636 (1994).
15. P. W. Anderson, *Phys. Rev. Lett.* **67**, 2092 (1991).
16. H. D. Drew, S. Wu, and H.-T. S. Linh, preprint.
17. B. Fisher, *et al.*, *J. Supercond.* **1**, 53 (1988); J. Genossar, *et al.*, *Physica C* **157**, 320 (1989).
18. S. Tanaka, *et al.*, *J. Phys. Soc. Japan* **61**, 1271 (1992).
19. K. Matsuura, *et al.*, *Phys. Rev. B* **46**, 11923 (1992); S. D. Obertelli, *et al.*, *ibid.*, p. 14928; C. K. Subramaniam, *et al.*, *Physica C* **203**, 298 (1992).
20. J. Kondo, *Prog. Theor. Phys.* **29**, 1 (1963).
21. Y. J. Uemura, *et al.*, *Phys. Rev. Lett.* **62**, 2317 (1989).
22. Ch. Niedermayer, *et al.*, *Phys. Rev. Lett.* **71**, 1764 (1993).